

Anti-lock braking control design for electric vehicles using LPV methods

Balázs Németh, Máté Fazekas and Péter Gáspár

Abstract—The paper proposes a novel Linear Parameter-Varying (LPV) based control approach for the anti-lock braking (ABS) functionality of electric vehicles. Through the advanced control design the hydraulic actuation and the regenerative braking of the electric motor can be coordinated efficiently. In the proposed control architecture the advantages of the different interventions can be combined, such as the the high torque generation capability of the hydraulic system and the fast actuation of the electric motor. The results of the LPV-based control design is presented through simulations using the high-fidelity CarMaker software.

I. INTRODUCTION AND MOTIVATION

Electro-mobility is a growing area in the field of automotive and vehicle dynamic research. Since the electric propulsion technology is a viable solution for the future challenges of the transportation problems [1], several R&D centers and institutes work on the control technologies of electric vehicles [2].

Several methods in the field of braking control for electric vehicles have been developed. A survey about the recent methods is found in [2]. It presents that the most common design methods for anti-lock braking control (ABS) are the rule-based control, the fuzzy approaches and the PID techniques. In [3] a linear quadratic control concept for slip control of anti-lock braking systems is proposed. An analysis about the optimal brake torque generation for ABS purposes is found in [4]. This paper proposes a polynomial-based method, by which the nonlinearity and the parameter-dependence of the braking dynamics can be incorporated in the control and its examination. [5] presents a further analysis, in which three different ABS concepts are compared to each other. The result of the examination is a regenerative slip tracking ABS control method, which guarantees better driving comfort due to the reduction of the deceleration oscillation. A sensorless ABS control concept for electric vehicles is presented in [6]. The advantage of the solution is that it omits the need for installation of separate conventional ABS sensors at each corner of the vehicle. An advanced iterative learning brake control concept for hybrid and electric vehicles is presented in [7]. In [8] an ABS control strategy for electric vehicles with in-wheel motors is found. An LPV control design method for two-wheeled vehicles equipped

with electromechanical front wheel brakes was proposed by [9].

An advantage of the electric vehicles is the possibility of regenerative braking. Through this functionality the motion energy of the vehicle can be recuperated efficiently, which results in a reduced energy consumption. Although the generated electric energy from the small vehicle deceleration can be stored in the battery of the automobile, the high deceleration can provide increased current during a short time. Thus, the high value of electric energy cannot be recuperated through the electric system. Moreover, the enlarged braking torque cannot be generated by the electric motor individually. Despite, a conventional hydraulic brake system is able to produce enough torque. Therefore, the combined actuation of hydraulic system and electric motor can be an appropriate choice for the braking functionality of electric vehicles.

From control engineering viewpoint the torque division between the interventions is a challenge of the design. Although the electric motor can generate only limited braking torque, it can be controlled more precisely, compared to the torque control of the hydraulic system. Furthermore, an advantage of the electric braking is its fast dynamics, by which the overall braking torque can be rapidly varied. In the coordination of the hydraulic brake system and the electric motor it is recommended to use the hydraulic system to generate high torque. Moreover, the goal of the electric motor is to guarantee the minimization of the error in the required torque generation.

As a novelty, in this paper a Linear Parameter-Varying (LPV) control for the design of ABS functionality of electric vehicles is presented. In the proposed solution the hydraulic braking and regenerative braking are coordinated, in which the advantages of the different actuators are incorporated. The LPV method can guarantee the coordination through the frequency-dependent weighting in the control design process. Moreover, the proposed solution is robust against the noises on the wheel speed sensors.

The paper is organized as follows. In Section II the control-oriented modeling of the braking system is presented. The resulted model is verified through CarMaker simulations. The LPV-based control design is found in Section III. It contains the description of the performances, process of the weighting in the control design and the optimization problem. The efficiency of the control design is found in Section IV, which presents CarMaker simulation results about the ABS control. Finally, the contributions of the paper is summarized in Section V.

B. Németh, M. Fazekas and P. Gáspár are with Systems and Control Laboratory, Institute for Computer Science and Control, Hungarian Academy of Sciences, Kende u. 13-17, H-1111 Budapest, Hungary. E-mail: [balazs.nemeth;mate.fazekas;peter.gaspar]@sztki.mta.hu

This work has been supported by the GINOP-2.3.2-15-2016-00002 grant of the Ministry of National Economy of Hungary.

II. MODELING THE BRAKING DYNAMICS

In the followings the control-oriented model of the combined hydraulic and electric braking system is presented. The modeling of braking dynamics is based on a one wheel model, which is loaded with one quarter of the vehicle mass.

The dynamics of the rotating wheel is formulated as

$$J\dot{\omega} = F_x r - T_{em} - T_{hyd}, \quad (1)$$

where J is the inertia of the wheel, ω is the rotating speed and r is the effective radius of the wheel. In the rotation dynamics F_x represents the longitudinal force between the tyre and the wheel, while T_{em} and T_{hyd} are the torque interventions of the electric motor and the hydraulic brake.

The longitudinal wheel slip λ is calculated as

$$\lambda = \frac{v - r\omega}{v}, \quad (2)$$

where v is the longitudinal velocity of the vehicle. The derivative of the slip λ is formed as

$$\dot{\lambda} = \frac{(\dot{v} - r\dot{\omega})v - (v - r\omega)\dot{v}}{v^2}. \quad (3)$$

Considering that the sampling time of the actuation in the ABS is very small, the impact of the vehicle velocity variation can be omitted. Thus, the approximation $\dot{v} = 0$ is considered in practice. It results in that (3) is transformed as

$$\dot{\lambda} = -\frac{r\dot{\omega}}{v}. \quad (4)$$

The longitudinal force F_x depends on several factors, such as λ , the vertical load on the wheel F_z and the μ parameter, which represents the surface between the tyre and the road. Although the relationships between these factors and F_z are nonlinear [10], the characteristics can be effectively linearized around $\lambda = 0$, such as

$$F_x = c\lambda\mu F_z \quad (5)$$

where c is a tyre coefficient, which represents the slope of the characteristics. Moreover, in the control-oriented model F_z considered as constant parameters and the road surface is considered to be homogenous with constant μ .

The dynamics of the longitudinal slip for control purposes is resulted by the relationships (1), (4) and (5):

$$\dot{\lambda} = -\frac{r}{v} \frac{c\lambda\mu F_z r - T_{em} - T_{hyd}}{J}. \quad (6)$$

The formed one-wheel model is validated through CarMaker simulations. During the simulations different constant brake torque values are generated at the ABS braking scenarios. The tyre model parameter c is identified from the CarMaker simulations, focusing on the signal of the longitudinal slip. The computed c parameter is applied in the LPV model (9), and the results of the simulations are compared to each other. Figure 1 shows the results of the simulations, such as the error in the steady-state longitudinal slip signal and its relative error. The results illustrate that the formed control-oriented LPV model (9) is able to approximate the high-fidelity model appropriately.

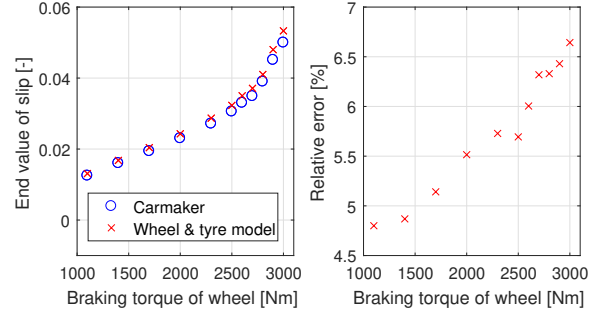


Fig. 1. Comparison of the CarMaker and the LPV models

Modeling the dynamics of brake actuation

Modeling of the hydraulic brake actuation is a complex problem due to the several nonlinearities of the hydraulic components and their various structures [11], [12]. In this paper the aim of the brake actuation modeling is to approximate the generation of the braking torque. Thus, it is necessary to find a transfer function between the reference torque defined by the braking controller and the realized wheel brake torque. In this paper a second-order form is chosen, such as

$$G_{hyd}(s) = \frac{T_{hyd}(s)}{T_{hyd,req}(s)} = \frac{1}{(T_{hyd1}s + 1)(T_{hyd2}s + 1)} \quad (7)$$

where $T_{hyd,req}$ is the required hydraulic braking torque, which is computed by the ABS controller. Furthermore, T_{hyd1}, T_{hyd2} are the parameters of the system. The parameters of the brake model are identified through CarMaker simulations, in which an enhanced hydraulic brake actuator model is applied. An illustration of the approximation is found in Figure 2. It shows that the complex braking actuation can be approximated suitable through the selected second-order model.

Another actuator of the braking system is the electric motor. There are several electric drivetrain constructions, depending on the construction and the traction concepts of the vehicle [13]. Electric motor can be used as an additional element in a hybrid drivetrain, see e.g. [14], [15]. It can be also used in a full electric vehicle for throttle with differential gear [16]. Furthermore, there are in-wheel motor solutions, respectively [17], [18]. In this paper it is assumed that the electric motor is able to generate torque directly on the wheels, but the architecture of the system can be varied. For modeling purposes a first-order transfer function form is selected, which represents the relationship between the required electric torque $T_{em,req}$ and the realized torque T_{em} :

$$G_{em}(s) = \frac{T_{em}(s)}{T_{em,req}(s)} = \frac{1}{(T_{em1}s + 1)}, \quad (8)$$

where T_{em1} is the time constant. Note that the generation of the braking torque is very fast, which means that the value of T_{em1} is in millisecond range. The step response of the system is illustrated in Figure 2. It can be seen that the response of the electric motor is significantly faster than the hydraulic system.

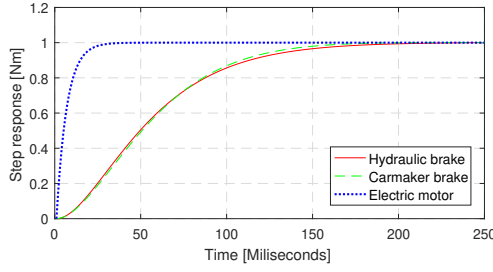


Fig. 2. Step responses of the actuators

III. LPV-BASED CONTROL DESIGN OF THE BRAKING SYSTEM

In this section the coordinated control design of the hydraulic and electric braking systems is presented. First, the LPV formulation and the performances are introduced. Second, the optimal control design process is presented.

A. LPV formulation and performances

The LPV control design of the system is based on the control-oriented slip dynamics of the vehicle, see (6). In the formulation the longitudinal velocity of the vehicle v is selected as a scheduling variable of the LPV system, because its variation has a high impact on the slip dynamics. Therefore, the representation is formed as

$$\dot{x} = A(\rho_1)x + B(\rho_1)u, \quad (9)$$

where ρ_1 is equivalent with the longitudinal vehicle speed v , the state vector contains the longitudinal slip of the wheel $x = [\lambda]$ and the control inputs are the hydraulic and the electric brake torques $u = [T_{hyd,req} \ T_{em,req}]^T$. The matrices $A(\rho)$ and $B(\rho)$ are as follows

$$A = \begin{bmatrix} -\frac{F_z r^2}{J \rho_1} c \end{bmatrix}, \quad (10a)$$

$$B = \begin{bmatrix} \frac{r}{J \rho_1} & \frac{r}{J \rho_1} \end{bmatrix}. \quad (10b)$$

The goal of the ABS control is to reach the maximum longitudinal braking force. It requires that the wheel must be kept in an optimal slip range. Therefore, the performance specification of the control system is to minimize the difference between the longitudinal slip of the wheel and the reference slip:

$$z_1 = \lambda_{ref} - \lambda \quad |z_1| \rightarrow \min, \quad (11)$$

where λ_{ref} is resulted from the characteristics of the tyre. The reference longitudinal slip is related to the maximum value of F_x .

Moreover, the coordination of the control inputs requires to find a balance between the control inputs $T_{hyd,reg}$ and $T_{em,reg}$. It can be reached to select the minimization of these signals as performances:

$$z_2 = T_{hyd,reg} \quad |z_2| \rightarrow \min, \quad (12a)$$

$$z_3 = T_{em,reg} \quad |z_3| \rightarrow \min. \quad (12b)$$

The performances are compressed to a performance vector, such as $z = [z_1 \ z_2 \ z_3]^T$.

Finally, the plant is based on the state-space representation (9) with the consideration of z . The system with the performance and the measurement relations is formed as

$$\dot{x} = A(\rho_1)x + B(\rho_1)u \quad (13a)$$

$$z = C_1 x + D u \quad (13b)$$

$$y = C_2 x \quad (13c)$$

The measured signal of the system is the slip λ , which is calculated from (2).

B. LPV-based control design

In the following the design of the LPV controller based on (13) is presented. The goal of the LPV method is to coordinate the actuation of the hydraulic and the electric brake system. In this coordination the dynamic properties must be considered to reach maximum longitudinal braking force. Therefore, weighting functions are used to scale the performance variables and some other signals. The aim of these weighting functions is to guarantee the balance between the interventions according to the dynamics of the actuators. The closed-loop architecture of the system with the weights is illustrated in Figure 3.

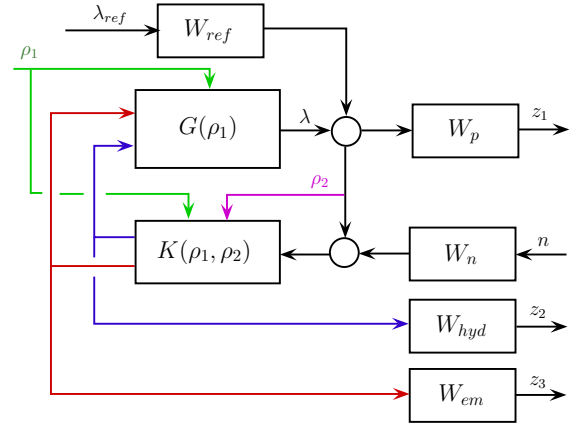
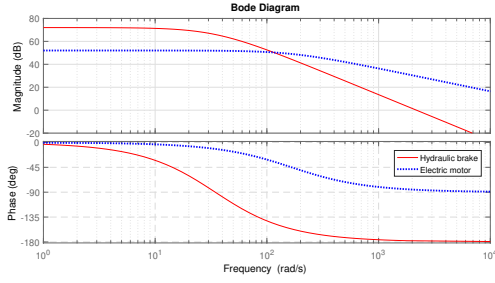


Fig. 3. Closed-loop interconnection scheme

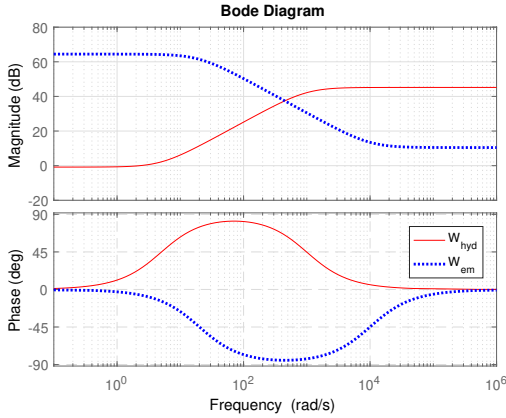
In the scheme, the performance z_1 is guaranteed by the weighting function W_p . The performance signals of the control interventions are weighted through the functions

$$W_i = G_i(\rho_2) \frac{A_{i1}s + A_{i0}}{T_{i1}s + T_{i0}}, \quad (14)$$

where index i is related to $i = \{hyd; em\}$ and A_{i1}, A_{i0}, T_{i1} and T_{i0} are design parameters. The selection of these parameters represent the frequency characteristic of the actuators, see Figure 4(a). The parameters must guarantee that the hydraulic actuator can generate the major part of the required torque, but only on lower frequencies, while the electric actuator can have high frequency intervention with smaller amplitude. The forms of the functions are found in Figure 4(b).



(a) Bode diagrams of the actuators



(b) Bode diagrams of the weighting functions

Fig. 4. Bode diagrams for the control design

Moreover, for the control design of the ABS functionality, another scheduling variable is selected, as found in Figure 3. The aim of $\rho_2 = |\lambda_{ref} - \lambda|$ is to avoid the saturation of the electric motor. For example at rapid brake pedal activation the slip error is significantly increased. This sudden change appears in the error signal as a high frequency effect, therefore the controller the electric motor is activated. However, the actuation of the electric motor is limited, which means that it is unable to generate the overall braking moment individually. It results in the saturation of the electric motor, which must be avoided. Therefore, $G(i)$ is formed as

$$G_i(\rho_2) = 1 + P_i \rho_2 \quad (15)$$

where P_i is a tuneable constant parameter.

Figure 3 contains two further weights. The role of W_{ref} is to scale the reference signal λ_{ref} , while W_n is related to the sensor noise n on the wheel velocity measurement.

The control design is based on the LPV method that uses single Lyapunov functions. The quadratic LPV performance problem is to choose the parameter-varying controller $K(\rho_1, \rho_2)$ in such a way that the resulting closed-loop system is quadratically stable and the induced \mathcal{L}_2 norm from the disturbance $w = [\lambda_{ref} \ n]^T$ and the performances z is less than the value γ . The minimization task is the following [19]:

$$\inf_K \sup_{\rho \in \mathcal{F}_P} \sup_{\|w\|_2, w \in \mathcal{L}_2} \frac{\|z\|_2}{\|w\|_2}, \quad (16)$$

where \mathcal{F}_P denotes the range of the scheduling variables. The existence of a controller that solves the quadratic LPV γ -performance problem can be expressed as the feasibility of a set of Linear Matrix Inequalities, which can be solved numerically. Finally, the state space representation of the LPV control $K(\rho_1, \rho_2)$ is constructed, see [20].

IV. SIMULATION RESULTS

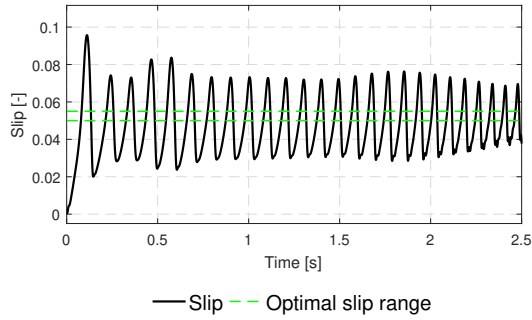
In this section the efficiency of the coordinated ABS control method is proposed through simulation scenarios. The results are performed through the high-fidelity vehicle dynamics software CarMaker, in which a conventional electric passenger car is selected. In the simulations at $v = 100$ km/h the brake pedal is fully pushed suddenly, which results in the activation of the braking actuators with anti-lock functionality. The goal of the simulations is to show that the LPV-based control is able to guarantee the longitudinal slip ratio of a single wheel at the maximum longitudinal force. The possible yaw-moment is neglected with the CarMaker driver settings. Thus, the proposed algorithm can guarantee maximum deceleration of the electric vehicle during the braking process.

In the simulation scenarios the reference longitudinal slip is selected as $\lambda_{ref} \equiv 0.05$. Moreover, in all cases a random noise is considered to be on the measurement of the wheel velocity. The saturation limits of the electric motor is ± 400 Nm, while it is between $0 \dots 4000$ Nm in case of the hydraulic torque.

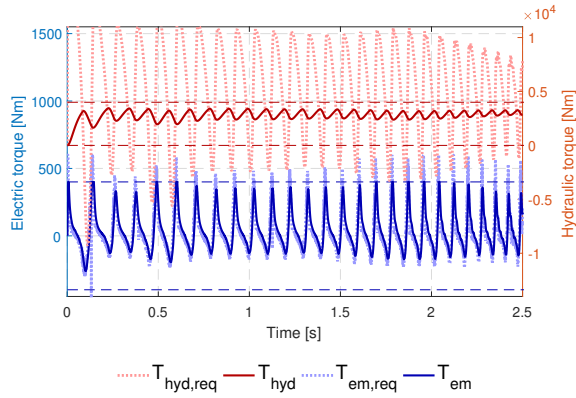
In the first simulation $P_{hyd} = P_{em} = 0$ of (15) is selected, which means that the saturation of the control actuation is not considered. It can be seen that it results in oscillation in the slip, as illustrated in Figure 5(a). Its reason is that at the beginning of the braking process the controller actuates the electric motor significantly due to the rapid brake pedal activation, as detailed in Section III. It results in the saturation of the electric motor and the hydraulic brake too, see Figure 5(b). Although the controller requires 500 Nm from the electric motor and more than 10000 Nm from the hydraulic system, these signals in the physical system cannot be guaranteed. Therefore, the incorporation of ρ_2 in the control design is required to avoid the unwanted effects of the saturation.

In the second simulation the scheduling variable ρ_2 is considered in the design, as proposed in (15). In this case the saturation of the control interventions is avoided, see Figure 6(b). The results show the impact of the weighting in the control, which means that the hydraulic actuator produces high torque and fast actuation by the electric motor. In Figure 6(c) the sum of the torques is founded. Using the electric motor as an additional brake actuator with the conventional hydraulic brake results in smoothed wheel torque, which can provide fast setting up to the optimal slip range. Therefore, the longitudinal slip is smooth and the tracking error is small, see Figure 6(a).

In the third simulation a white noise disturbance between $0.5 - 2$ sec is added to the output of the hydraulic actuator. It represents the difference from the ideal behavior of the



(a) Longitudinal slip



(b) Braking torques

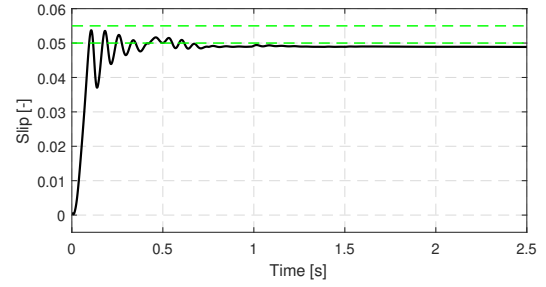
Fig. 5. Simulation scenario without saturation avoidance (dotted red line: $T_{hyd,req}$, solid red line: T_{hyd} , dotted blue line: $T_{em,req}$, solid blue line: T_{em})

hydraulic actuator due to the uncertainties of the actuator. The disturbance can be seen in Figure 7(c). Through the appropriate selection of the the weighting functions in the LPV control, the coordination of the interventions is able to eliminate the effects of the disturbance. This is due to the rapid dynamics of the electric motor, which is able to reject the disturbance effects, see Figure 7(b). Therefore, the slip error is minimized efficiently, which results in λ around the maximum braking force, see Figure 7(a). Figure 7(d),(e) show that the variation of the electric motor torque is significantly higher than the variation of $T_{hyd,req}$. It demonstrates that the controller actuates mostly the electric motor at the high frequency range, while the hydraulic system guarantees the high torque.

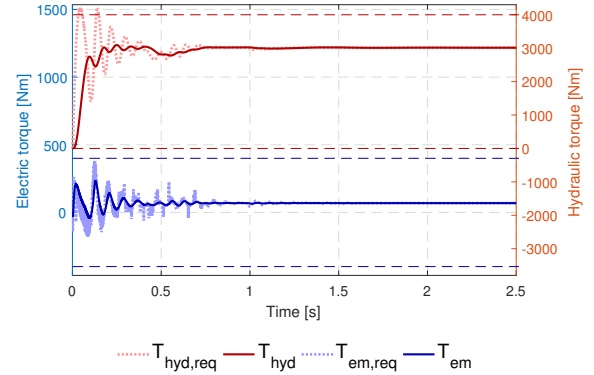
The simulation scenarios demonstrate that the proposed LPV control is able to guarantee the required slip value, by which the maximum deceleration can be generated. The advantages of the actuators can be utilized through the coordination, which has been built-in the control design.

V. CONCLUSIONS

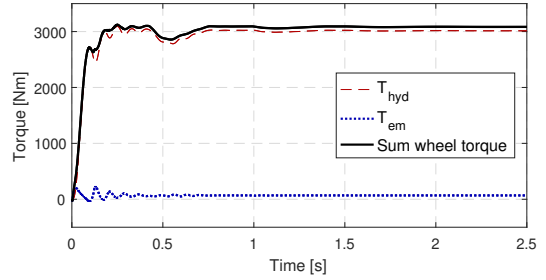
The paper proposed an LPV-based coordinated control strategy of electric vehicles for anti-lock braking functionality. The control-oriented model of the system was presented



(a) Longitudinal slip



(b) Braking torques



(c) Sum of the braking torques

Fig. 6. Simulation scenario with saturation avoidance

and formulated in a parameter-dependent form. In the control design the advantages of the different actuators were incorporated in, such as the high torque generation capability of the hydraulic system and the fast dynamics of the electric motor. The efficiency of the control structure was presented through CarMaker simulations.

As a future challenge, the efficiency of the control system can be improved through the more precise estimation of the tyre characteristics. Since the tyre model parameters have high impacts on the intervention, the estimation of their actual values can improve the preciseness of the slip control. Moreover, the braking of the four wheels can result in yaw moment on the vehicle chassis. The avoidance of the unnecessary effect requires an enhanced control strategy and the coordination with further control systems, which will be discussed in the further research.

REFERENCES

- [1] K. Rajashekara, "Present status and future trends in electric vehicle propulsion technologies," *IEEE Journal of Emerging and Selected Topics in Power Electronics*, vol. 1, no. 1, pp. 3–10, March 2013.
- [2] V. Ivanov, D. Savitski, and B. Shyrokau, "A survey of traction control and antilock braking systems of full electric vehicles with individually controlled electric motors," *IEEE Transactions on Vehicular Technology*, vol. 64, no. 9, pp. 3878–3896, Sept 2015.
- [3] M. Ringdorfer and M. Horn, "Development of a wheel slip actuator controller for electric vehicles using energy recuperation and hydraulic brake control," in *2011 IEEE International Conference on Control Applications (CCA)*, Sept 2011, pp. 313–318.
- [4] B. Németh, P. Gáspár, and J. Bokor, "Analysis of braking dynamics using parameter-dependent polynomial Control Lyapunov Functions," in *53rd IEEE Conference on Decision and Control*, Dec 2014, pp. 2536–2541.
- [5] D. Savitski, V. Ivanov, and B. Shyrokau, "Experimental investigations on continuous regenerative anti-lock braking system of full electric vehicle," *Int.J. Automat. Technol.*, vol. 17, no. 2, pp. 327–338, 2016.
- [6] A. Dadashnialehi, A. Bab-Hadiashar, Z. Cao, and A. Kapoor, "Intelligent sensorless antilock braking system for brushless in-wheel electric vehicles," *IEEE Transactions on Industrial Electronics*, vol. 62, no. 3, pp. 1629–1638, March 2015.
- [7] C. Mi, H. Lin, and Y. Zhang, "Iterative learning control of antilock braking of electric and hybrid vehicles," *IEEE Transactions on Vehicular Technology*, vol. 54, no. 2, pp. 486–494, March 2005.
- [8] Y. Yang, S. Yang, L. Yang, and Y. Liu, "A new abs control strategy designed for electric vehicle independently driven by four wheel motors," in *Proceedings of the 2nd International Conference on Computer Science and Electronics Engineering*. Atlantis Press, 2013, pp. 1264–1267.
- [9] M. Corno, S. M. Savaresi, and G. J. Balas, "Linear Parameter-Varying wheel slip control for two-wheeled vehicles," in *2008 47th IEEE Conference on Decision and Control*, Dec 2008, pp. 5030–5035.
- [10] R. Rajamani, "Vehicle dynamics and control," *Springer*, 2005.
- [11] M. L. Kuang, M. Fodor, D. Hrovat, and M. Tran, "Hydraulic brake system modeling and control for active control of vehicle dynamics," in *Proceedings of the 1999 American Control Conference (Cat. No. 99CH36251)*, vol. 6, 1999, pp. 4538–4542.
- [12] J. Gerdes and J. Hedrick, "Brake system modeling for simulation and control," *ASME. J. Dyn. Sys., Meas., Control.*, vol. 121, no. 3, pp. 496–503, 1999.
- [13] A. Emadi, Y. J. Lee, and K. Rajashekara, "Power electronics and motor drives in electric, hybrid electric, and plug-in hybrid electric vehicles," *IEEE Transactions on Industrial Electronics*, vol. 55, no. 6, pp. 2237–2245, June 2008.
- [14] M. Zeraoulia, M. E. H. Benbouzid, and D. Diallo, "Electric motor drive selection issues for hev propulsion systems: A comparative study," *IEEE Transactions on Vehicular Technology*, vol. 55, no. 6, pp. 1756–1764, Nov 2006.
- [15] S. G. Wirasingha, N. Schofield, and A. Emadi, "Plug-in hybrid electric vehicle developments in the us: Trends, barriers, and economic feasibility," in *2008 IEEE Vehicle Power and Propulsion Conference*, Sept 2008, pp. 1–8.
- [16] G. Rizzoni, *Powertrain Control for Hybrid-Electric and Electric Vehicles*. London: Springer London, 2013, pp. 1–10.
- [17] H. Shimizu, J. Harada, C. Bland, K. Kawakami, and L. Chan, "Advanced concepts in electric vehicle design," *IEEE Transactions on Industrial Electronics*, vol. 44, no. 1, pp. 14–18, Feb 1997.
- [18] S. Murata, "Innovation by in-wheel-motor drive unit," *Vehicle System Dynamics*, vol. 50, no. 6, pp. 807–830, 2012.
- [19] J. Bokor and G. Balas, "Linear Parameter Varying Systems: A geometric theory and applications," *16th IFAC World Congress, Prague*, 2005.
- [20] F. Wu, "A generalized LPV system analysis and control synthesis framework," *Int.J. Control*, vol. 74, pp. 745–759, 2001.

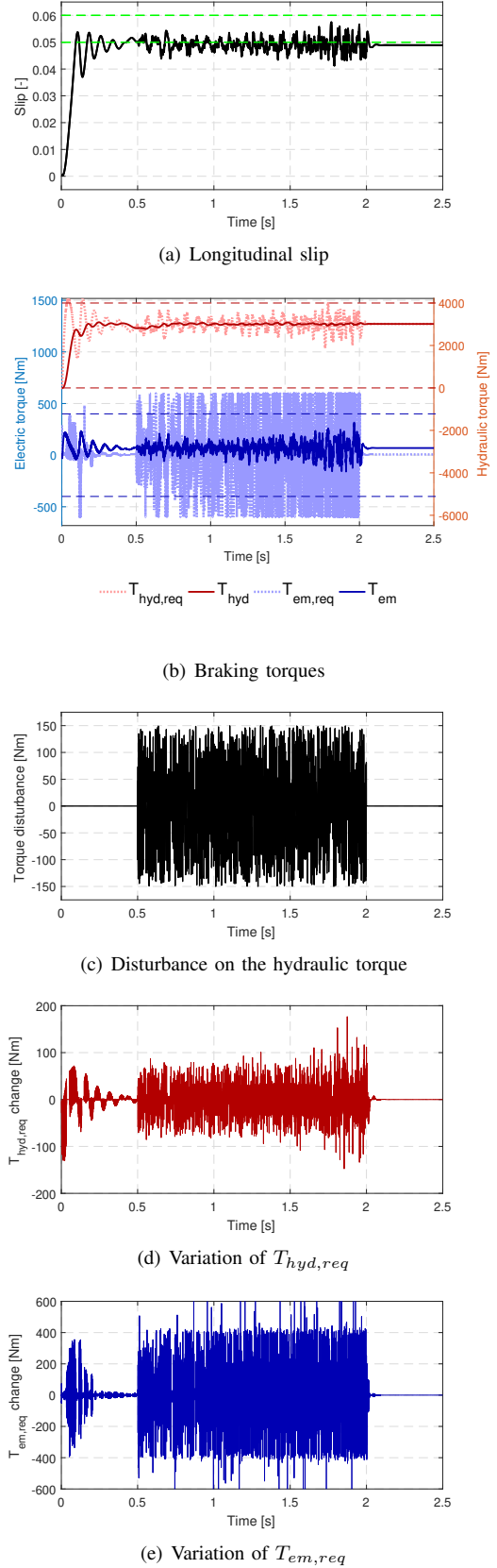


Fig. 7. Simulation scenario with the disturbances of the hydraulic actuator